PAPER

Check for updates

Photoluminescence, thermal and surface properties of triarylimidazole-containing polyimide nanocomposite films

Wu Bai,[a] Yunhua Lu, [iD] *[a] Zhizhi Hu,*[ab] Guoyong Xiao,[a] Hongbin Zhao,[ab] Jianmin Zhu[b] and Zhaobin Liu[b]

In this work, a triarylimidazole-containing diamine 2-(4-methylphenyl)-4,5-bis(4-(4-amino-2-trifluoromethylphenoxy)phenyl)imidazole (MPBAI) was firstly synthesized and polymerized with 1,2,3,4-cyclobutanetetracarboxylic dianhydride (CBDA) to prepare transparent polyimide (PI) films by means of thermal imidization. Then, inorganic nanoparticles including silica (SiO_2), alumina (Al_2O_3) and silicon nitride (Si_3N_4) were separately introduced into the PI(MPBAI-CBDA) with different mass fractions of 0.02%, 0.10%, 0.50% and 2.50% to obtain three series of PI nanocomposite films. All these films were close to colorless and transparent, although the light transmittance showed a downward trend due to the introduction of nanoparticles. Moreover, as the content of inorganic nanoparticles increased, the fluorescence intensities of these films were increased. Comparatively, the improvement effect of nano-SiO_2 was the most obvious. When the content of SiO_2 was 2.50%, the maximum intensity of the fluorescence absorption peak was increased by 9.6 times, and the absolute fluorescence quantum yield reached 17.2%, about 5.2 times that of the original PI film. Moreover, the maximum absorption peak produced a red shift of 85 nm due to the addition of 2.50% Si_3N_4, which was probably caused by the weakening of fluorescence quenching effect and high permittivity. The nanocomposites exhibited high glass transition temperatures of around 300 °C and excellent thermal stabilities. The surface hydrophobicity was changed by adjusting the mass and type of nanoparticles. Thus, this work provided a simple way to improve the photoluminescence effect by introducing the nanoparticles. The functional films will be expected to be applied in some optical applications.

1. Introduction

Polyimide (PI) has excellent thermal and mechanical properties and chemical solvent resistance, and has been widely used in electrical and electronic equipment, aerospace, separation and other fields.[1–6] Because the traditional aromatic PI is brownish-yellow in color due to the visible absorptance of charge transfer complex (CTC) formed between dianhydrides and diamines, which limits its application in optical fields.[7,8] In recent years, many researchers have made great efforts to improve the optical properties of PI films, such as the introduction of $-CF_3$ group, alicyclic structure, non-coplanar and twisted structure.[9–11] The PI film with high temperature resistance, colorless and transparent characteristics can be used as coating, protective layer, flexible displays and transparent circuit boards, *etc.*[12–16] Moreover, there has been a growing interest in functional PI film materials.[17–20] For instance, photoluminescence PI has attracted researchers' interest because of its unique luminescence

properties. According to some literatures, the PIs containing anthracene and oxadiazole structures show photoluminescence behavior, which can be applied as the light-emitting layer in electroluminescent devices.[21,22] Besides, imidazole structures are commonly used as luminescent group to endow PI with some photoluminescence properties.[23–29] However, the fluorescence quantum yields of these PIs need to be further increased to meet the practical applications.[30–32] Therefore, it is of great significance to propose some methods to prepare and improve the fluorescence properties, except molecular structure design.

Up to now, the introduction of nanoparticles to improve the properties of polymer materials has become a common modification method.[33–36] Nanoparticles, for example carbon nanotubes (CNT), graphene oxide (GO), SiO_2, Al_2O_3, ZnO, $CaCO_3$, Si_3N_4 and TiO_2, have the characteristics of small size effect, surface effect and quantum tunneling effect, which could provide polymer materials with the certain improvement, such as dielectric, thermal, mechanical properties and gas permeabilities.[37–40] It is noted that the content and type of nanoparticles take great effects on the properties of nanocomposites, and agglomeration phenomenon need to be avoided as soon as possible.[41,42] The proper addition of nanoparticles can

[a]School of Chemical Engineering, University of Science and Technology Liaoning, Anshan, Liaoning, P. R. China. E-mail: lee.lyh@163.com; huzhizhi@163.com
[b]Oxiranchem Holding Group Co. Ltd, Liaoyang, Liaoning, P. R. China

effectively improve the properties of the composites. Recently, the PI nanocomposites or mixed matrix membranes have been extensively studied, and some better modification results are obtained.[43] As for photoluminescent PI film materials, there are few studies on the modification of nanoparticles.[44] Commonly, the molecular chains of photoluminescent PI contain a large number of luminescent groups, but in solid film state, the luminescence intensity is relatively weak and the luminescence efficiency is low because of the quenching effect induced by the close arrangement of molecular chains.[45] The introduction of nanoparticles will weaken the ordered stacking state of PI molecular chains, enlarge the distance between molecular chains, and reduce the interaction between the chains. According to the literature,[46] the barium titanate nanoparticles with high permittivities could increase the fluorescence intensity of the ZnO–polymethylmethacrylate nanocomposite film. Hence, it is expected that the ceramics nanoparticles have a positive impact on the optical property of photoluminescent PI film.

In this work, the diamine containing triphenylimidazole structures 2-(4-methylphenyl)-4,5-bis(4-(4-amino-2-trifluoromethylphenoxy)phenyl)imidazole (MPBAI) was firstly synthesized and polymerized with 1,2,3,4-cyclobutanetetracarboxylic acid dianhydride (CBDA) to prepare the transparent and colorless PI film. Then, three kinds of ceramics nanoparticles including SiO_2, Al_2O_3, and Si_3N_4 were separately introduced into the PI(MPBAI-CBDA) matrix by *in situ* polymerization method to obtain nanocomposite films. The influence of content of nanofillers on the thermal, optical and surface properties was investigated. As a result, the fluorescence intensities of nanocomposite films were sharply enhanced due to the introduction of nanoparticles, although the optical transmittance relatively declined. And, the 2.50% nano-Si_3N_4 made the fluorescence emission peak produce an obvious red shift. Therefore, these nanocomposites exhibit excellent optical performance, which are expected to be used in flexible light-emitting devices, fluorescent sensors, plastic lasers, solar cells and light wave converters in the future.

2. Experimental

2.1 Materials

4,4′-Dihydroxydiphenylethylenedione, 4-methylbenzaldehyde, and 2-chloro-5-nitrobenzotrifluoride were purchased from Shanghai Aladdin Biochemical Technology Co., Ltd (China) and used directly without purification. 1,2,3,4-Cyclobutanetetracarboxylic dianhydride (CBDA) was provided by

Oxiranchem Holding Group Co. Ltd (China). Nano-SiO_2 of 99.5% (10–20 nm), nano-Al_2O_3 with the purity of 99.9% (γ phase, 5–15 nm) and 99.5% nano-Si_3N_4 (10–20 nm) were bought from Shanghai Aladdin Biochemical Technology Co., Ltd (China). Other reagents were obtained from Shanghai Macklin Biochemical Co., Ltd (China).

2.2 Synthesis of diamines

According to the literatures,[23–29] the synthesis steps of triphenylimidazole-containing diamines are shown in Scheme 1.

Synthesis of 4,4′-(4-nitro-2-trifluoromethylphenoxy) diphenylethylenedione (BNTFPED). 2-Chloro-5-nitrobenzotrifluoride of 45.561 g (0.202 mol) and 4,4′-dihydroxydiphenyl ethylenedione of 24.223 g (0.100 mol) were introduced into a 500 mL round flask with 100 mL dimethyl sulfoxide (DMSO). Under stirring, NaHCO$_3$ of 16.970 g (0.202 mol) was added to the mixture and reacted at 100 °C for 6 h. After cooled down, the brown solution was slowly poured into a large amount of deionized water with stirring. The precipitated light-yellow solid was filtered, washed for many times and dried under vacuum to obtain the crude product about 60.200 g. After recrystallized, the fine needle-like crystals were obtained with a yield of 88.0% and purity (HPLC) of 99.0%. ^{1}H NMR (500 MHz, DMSO-d_6, ppm): δ: 8.58 (s, 2H), 8.54 (d, J = 9.3 Hz, 2H), 8.09 (d, J = 8.2 Hz, 4H), 7.44 (t, J = 9.9 Hz, 6H). FTIR (KBr, cm^{-1}): 1668 (C=O), 1582, 1362 (NO$_2$), 1112 (C–O–C).

2-(4′-Methylphenyl)-4,5-bis(4-(4-nitro-2-trifluoromethylphenoxy)phenyl)imidazole (MPBNI). 6.008 g (0.050 mol) of 4-methylbenzaldehyde, 33.033 g (0.050 mol) of BNTFPED and 38.535 g (0.500 mol) of CH$_3$COONH$_4$ were placed into a 500 mL round flask containing 150 mL CH$_3$COOH. After the mixture was heated at 120 °C for 9 h, the solution was cooled down and slowly introduced into deionized water. The yellow crude product was separated and washed, followed by recrystallization. ^{1}H NMR (500 MHz, DMSO-d_6, ppm): δ: 12.74 (s, 1H), 8.54 (d, J = 12.3 Hz, 3H), 8.48 (d, J = 9.4 Hz, 1H), 7.99 (d, J = 7.1 Hz, 2H), 7.70 (dd, J = 19.9, 6.8 Hz, 4H), 7.33 (dd, J = 23.9, 7.3 Hz, 4H), 7.26–7.13 (m, 4H), 2.37 (s, 3H). FTIR (KBr, cm^{-1}): 1530, 1329 (NO$_2$), 3089 (N–H), 1622 (C=N), 1329 (C–N), 1114 (C–O–C).

2-(4-Methylphenyl)-4,5-bis(4-(4-amino-2-trifluoromethylphenoxy)phenyl)imidazole (MPBAI). 28.823 g (0.04 mol) MPBNI and 2.800 g Pd/C (10% Pd) were added to a 500 mL round flask with 200 mL absolute ethanol to carry out the reduction reaction. After heated to 70 °C, 28.8 mL hydrazine hydrate (85%) was slowly dripped into the solution and kept
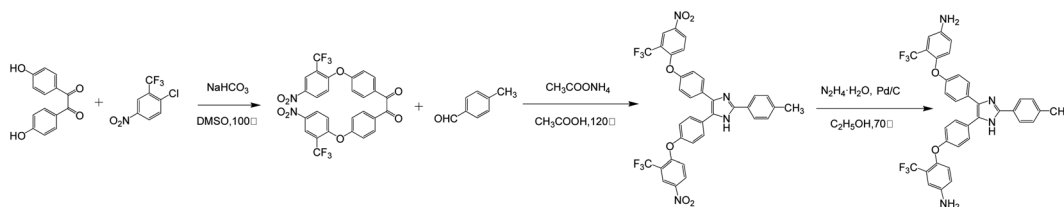
Scheme 1 Synthesis routes of the diamine MPBAI.

stirring for 6 h. After removing the catalyst by thermal filtration, the solvent was removed from the filtrate by rotary evaporation to obtain the white product with purity of 99%. ^{1}H NMR (500 MHz, DMSO-d_6, ppm): δ: 12.50 (s, 1H), 7.94 (d, J = 6.1 Hz, 2H), 7.56–7.41 (m, 4H), 7.27 (d, J = 7.1 Hz, 2H), 6.94 (d, J = 8.7 Hz, 5H), 6.83 (d, J = 6.8 Hz, 4H), 5.49 (d, J = 27.4 Hz, 4H), 2.35 (s, 3H). FTIR (KBr, cm^{-1}): 3380, 1629 (N–H), 1611 (C=N), 1336 (C–N), 1119 (C–O–C).

2.3 Preparation of triarylimidazole-containing PI and nanocomposite films

The triarylimidazole-containing PI films were prepared by solution polymerization and thermal imidization. First, the MPBAI monomer was added to the N,N-dimethyl acetamide (DMAc) solvent, stirring until completely dissolved. Then, the dianhydride CBDA was introduced into the above solution and stirred for 24 h to synthesize the poly(amic acid) (PAA) solution with a solid content of 15%. Next, the PAA was coated on a glass pane and thermally imidized in nitrogen atmosphere as follows: 80 °C/0.5 h, 120 °C/0.5 h, 160 °C/0.5 h, 200 °C/0.5 h, 250 °C/0.5 h and 300 °C/0.25 h. Finally, the film was stripped from the glass by immersion in water and dried at 100 °C for 24 h.

These nanocomposite films were fabricated by *in situ* polymerization method. First, the calculated and weighed nanoparticles, such as nano-SiO$_2$, Al$_2$O$_3$ and Si$_3$N$_4$ respectively placed into a certain amount of DMAc and dispersed under ultrasonic for 2 h. Next, the MPBAI and CBDA were successively added to the solution, and the further polymerization and thermal treatment were conducted according to the above process. The contents of nanoparticles in the PI matrix were set as 0.02%, 0.10%, 0.50% and 2.50% respectively, and three series of nanocomposite films were obtained (Scheme 2).

2.4 Characterization

The chemical structures of monomer and polymer films were characterized by Swiss Bruker AVANCE 500 MHz Nuclear Magnetic Resonance spectrometer (NMR) with dimethyl sulfoxide (DMSO) as the deuterated reagent and Nicolet IS10 Fourier transform infrared spectrometer (FT-IR) scanning from 500 to 4000 cm^{-1}. The microstructure of the films was investigated by PANalytical BLKII-5FF-SX X-ray diffractometer (XRD) in the range of 5–90°. The thermal properties were tested by PerkinElmer Pyris1 TGA thermal analyzer (TGA) at a heating rate of

20 °C min^{-1} from 30 to 800 °C and DMA 8000 Dynamic Mechanical Thermal Analyzer (DMTA) in the range of 50–400 °C with a heating speed of 5 °C min^{-1} in N$_2$. The optical transmittance and fluorescence properties of these films were measured by PerkinElmer Lambda 900 UV/Vis/NIR spectrophotometer and LS55 fluorescence/phosphorescence/luminescence spectrophotometer. The HORIBA/Fluorolog-3 fluorescence spectrometer with an integrating sphere was employed to test fluorescence quantum yield. The micromorphology of fracture section was sprayed by platinum and observed by Zeiss-IGMA HD Field Emission Scanning Electron Microscope (FE-SEM). The water contact angle on the surface of the samples was recorded with a ZJ-6900 optical contact angle measuring instrument. The water absorption was tested according to following method: a film sample was cut into 2 cm × 2 cm, wiped by absolute ethanol and dried at 120 °C for 12 h. After weighed accurately, it was immersed into deionized water in a tube for 24 h at room temperature. The residual water on the film surface was sucked by filter paper and weighed again. The water absorption was calculated by the following formula:

$$W = (m_{\text{wet weight}} - m_{\text{dry weight}})/m_{\text{dry weight}} \times 100\% \tag{1}$$

3. Results and discussions

3.1 Chemical structures of triarylimidazole-containing PI and nanocomposite films

According to our reported procedure,[47] the diamine MPBAI was synthesized and polymerized with alicyclic dianhydride CBDA to prepare the colorless and transparent PI film by thermal imidization. Next, the three series of nanocomposite films were fabricated by *in situ* polymerization using nano-SiO$_2$, Al$_2$O$_3$ and Si$_3$N$_4$ as inorganic nanofillers. In each nanocomposite films, the loadings of nanofillers were designed as 0.02%, 0.10%, 0.50% and 2.50%, respectively. Fig. 1 gives the FTIR spectra of PI(MPBAI-CBDA) and nanocomposite films, from which there are three characteristic peaks of imide ring at 1780, 1712 and 1372 cm^{-1}, corresponding to the asymmetric and symmetric stretching vibration of C=O group as well as the stretching vibration of C–N bond in the imide rings, respectively.[47] In addition, the vibration absorption peak of deformation for imide ring is observed at 720 cm^{-1}, and the C–O–C stretching
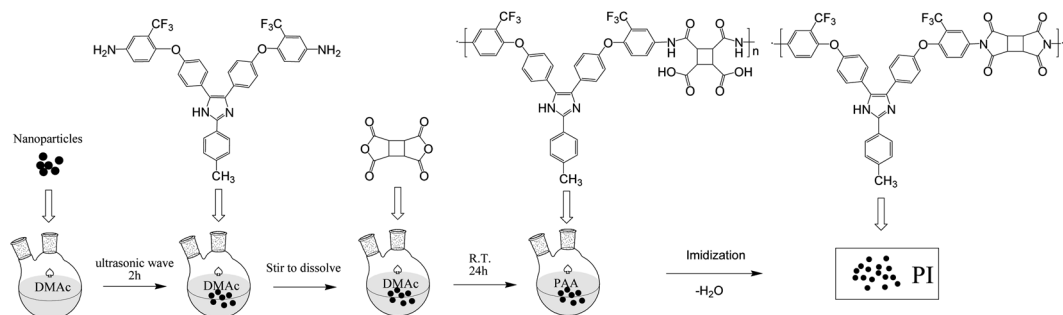
Scheme 2 Preparation of triarylimidazole-containing PI nanocomposite films.
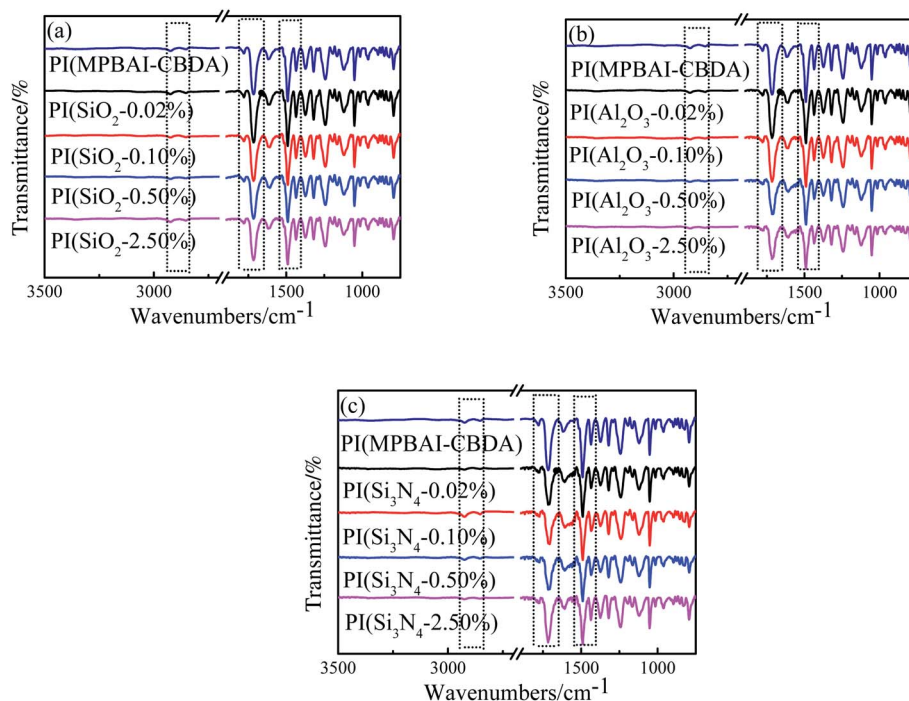
Fig. 1   FTIR spectra of triarylimidazole-containing PI and nanocomposite films.

absorption peak occurs around at 1245 cm^{-1}, which is assigned to the ether linkage in the PI backbone. Because the loading of nanoparticles was small, the chemical structures of the three ceramics nanofillers were not obviously reflected by the FTIR spectra. Generally, the FTIR spectra of PI(MPBAI–CBDA) and three series of nanocomposites are very similar, which indicates that these films contain imide ring structures.

3.2 Microstructure of crystallography

The FE-SEM images of fracture section of triarylimidazole-containing PI and nanocomposite films containing 2.50% inorganic ceramics fillers are shown in Fig. 2. It is observed that the fracture morphology of the prepared PI(MPBAI–CBDA) film is relatively dense and flat, which is mostly caused by brittle
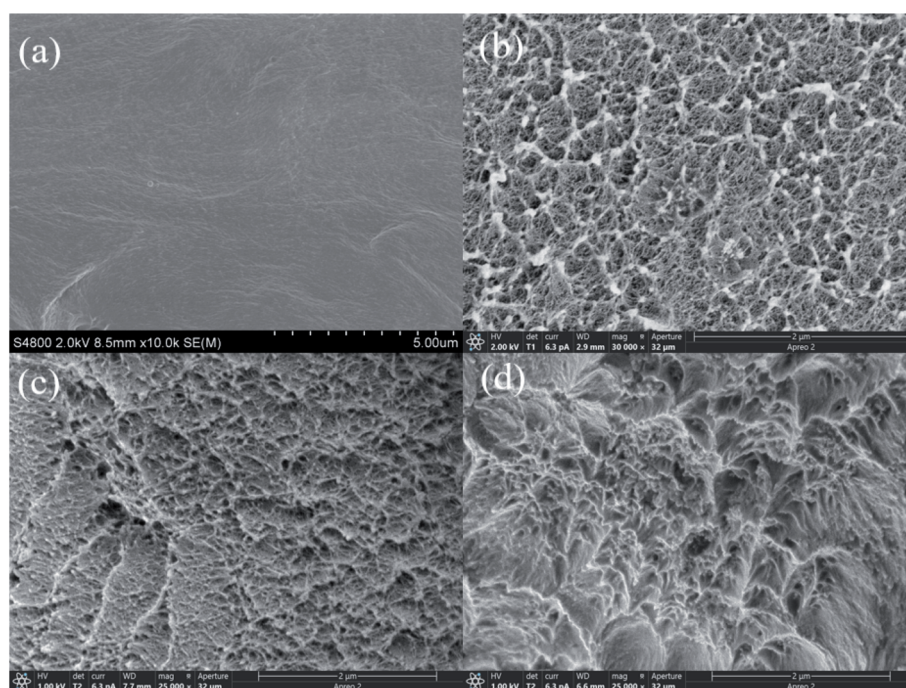

Fig. 2   SEM images of triarylimidazole-containing PI and nanocomposite films (a) PI(MPBAI–CBDA), (b) PI(SiO$_2$-2.50%), (c) PI(Al$_2$O$_3$-2.50%), (d) PI(Si$_3$N$_4$-2.50%).
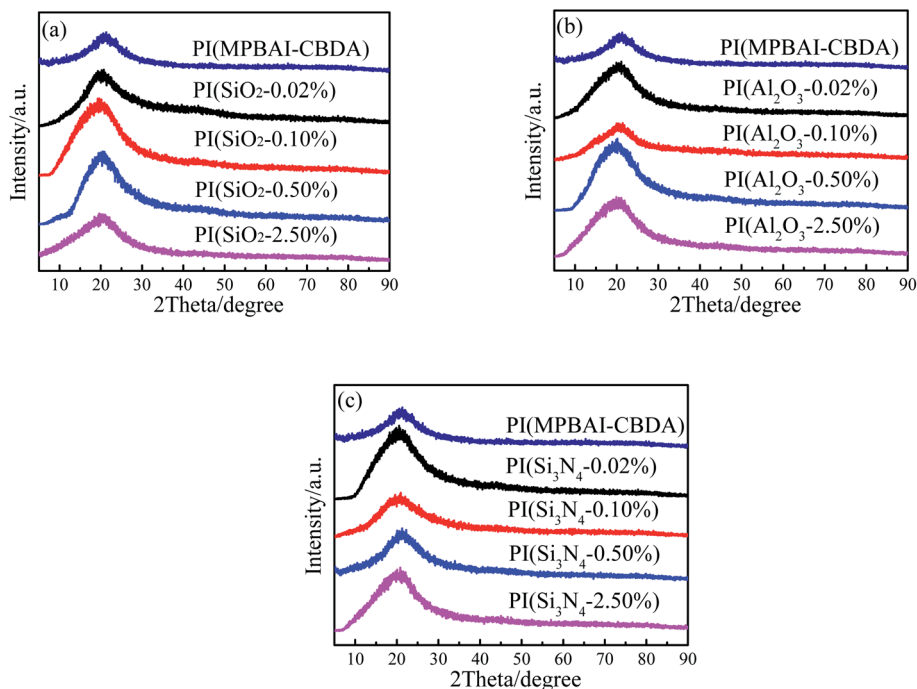
Fig. 3 XRD patterns of triarylimidazole-containing PI and nanocomposite films.

fracture. After adding the nanofillers, the significant difference can be seen in the surface morphology of nanocomposite films compared with pure PI film. From Fig. 2(b)–(d), the three fracture surfaces obviously become rough and uneven, which are ascribed to the toughening effect of nanofillers. It is well known that the nanoparticles in the polymer matrix could help to transfer the load, leading to the improvement of mechanical

properties. The reason for it is that some –OH groups on the surface of the ceramics nanoparticles are helpful to increase the interaction between the inorganic and organic phases.[48]

The crystallization performance of the triarylimidazole-containing PI and nanocomposite films was estimated by XRD, as given in Fig. 3. The diffraction peaks of these films are mainly concentrated near at 2 theta = 20.8°, corresponding to *d*-
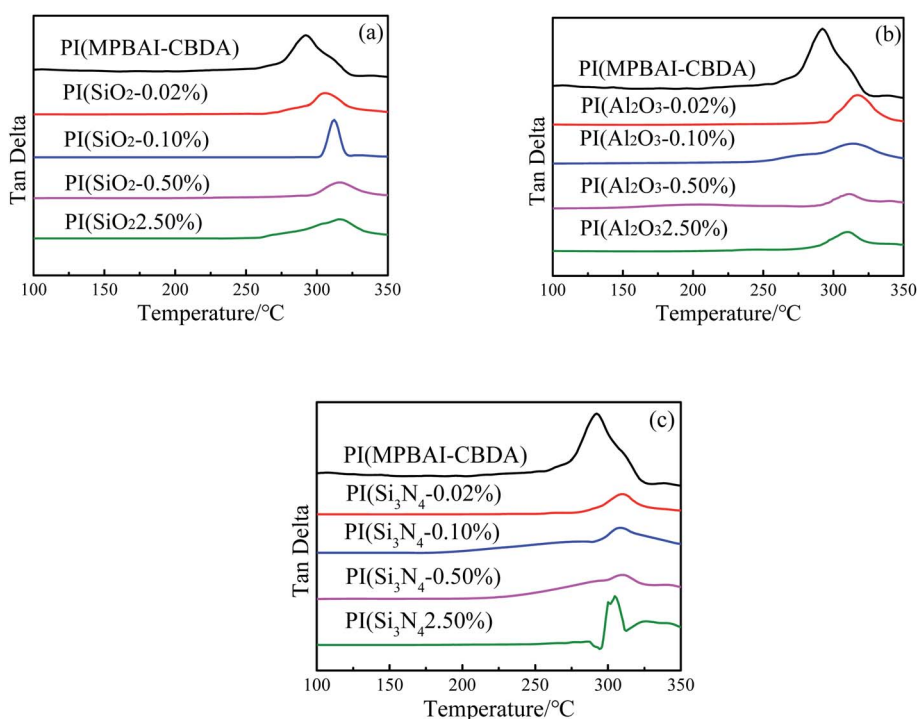

Fig. 4 DMTA curves of triarylimidazole-containing PI and nanocomposite films.

Table 1 Thermal and mechanical data of nano-doped polyimide film containing triarylimidazole[a]

| Samples	T_{d5} (°C)	T_{d10} (°C)	T_g (°C)	R_{800} (%)	W (%)	θ (°)	Thickness (μm)
PI(MPBAI-CBDA)	448.2	479.1	292.2	59.9	1.90	59	72
PI(SiO$_2$-0.02%)	445.0	495.6	305.8	63.4	1.98	64	84
PI(SiO$_2$-0.10%)	443.9	467.4	312.1	57.7	2.96	77	71
PI(SiO$_2$-0.50%)	442.2	478.9	317.1	61.9	3.03	79	74
PI(SiO$_2$-2.50%)	441.4	459.2	315.7	59.0	3.03	81	80
PI(Al$_2$O$_3$-0.02%)	444.7	479.0	317.1	60.2	2.96	75	55
PI(Al$_2$O$_3$-0.10%)	446.8	470.8	315.5	59.3	2.53	78	62
PI(Al$_2$O$_3$-0.50%)	446.1	476.6	310.9	61.8	1.94	81	61
PI(Al$_2$O$_3$-2.50%)	445.2	463.9	310.1	60.4	1.59	84	68
PI(Si$_3$N$_4$-0.02%)	441.3	470.5	310.6	59.8	1.98	64	60
PI(Si$_3$N$_4$-0.10%)	440.7	467.9	309.1	60.8	2.33	80	72
PI(Si$_3$N$_4$-0.50%)	440.3	479.5	308.3	62.3	2.61	83	65
PI(Si$_3$N$_4$-2.50%)	439.4	468.9	304.7	57.5	2.82	85	49

[a] T_{d5}: the temperature at which the mass loss is 5%, T_{d10}: the temperature at which the weight loss is 10%, R_{800}: the residual weight of the measured substance at 800 °C, T_g: glass transition temperature tested by DMTA, W: water absorption rate of film, θ: film contact angle, thickness: polyimide film thickness.

spacing of 0.427 nm. The gentle peak shape of pure PI film indicates the amorphous feature, which is probably ascribed to the irregular packing of PI molecular chains due to the existence of the large volume triarylimidazole groups. When the nanoparticles are doped, the position of the diffraction peaks slightly shifts to left at different degrees. The reason for it may be that the distance between the layers is probably enlarged because of the introduction of inorganic fillers. The diffraction patterns of nanocomposite films still show broad peak, illustrating the amorphous nature similar to the pure PI film. Moreover, the increase of diffraction peak intensity indicates the formation of short-range ordered structures induced by the nanoparticles. In the PI matrix, the three nanoparticles may act as nucleating agents to promote the regular arrangement of PI macromolecular chains.[49] In general, the three series of nanocomposite films exhibit similar change trend, which shows that the incorporation of nanofillers takes a certain effect on the microstructures of PI films.

3.3 Thermal properties

The thermal properties of triarylimidazole-containing PI and nanocomposite films were evaluated by DMTA and TGA (in Fig. 4), and the corresponding data are listed in Table 1. It can
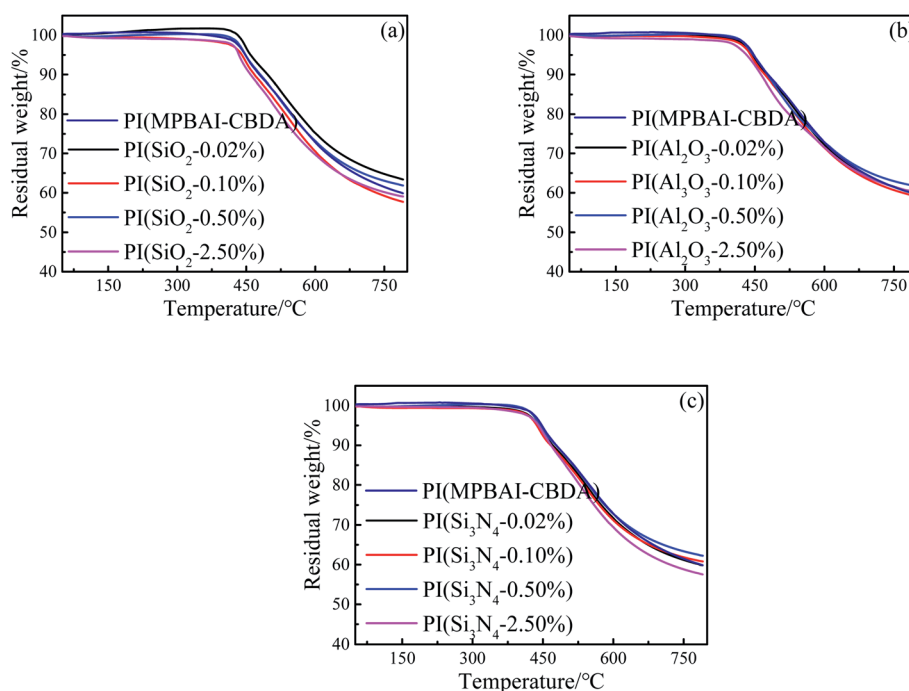
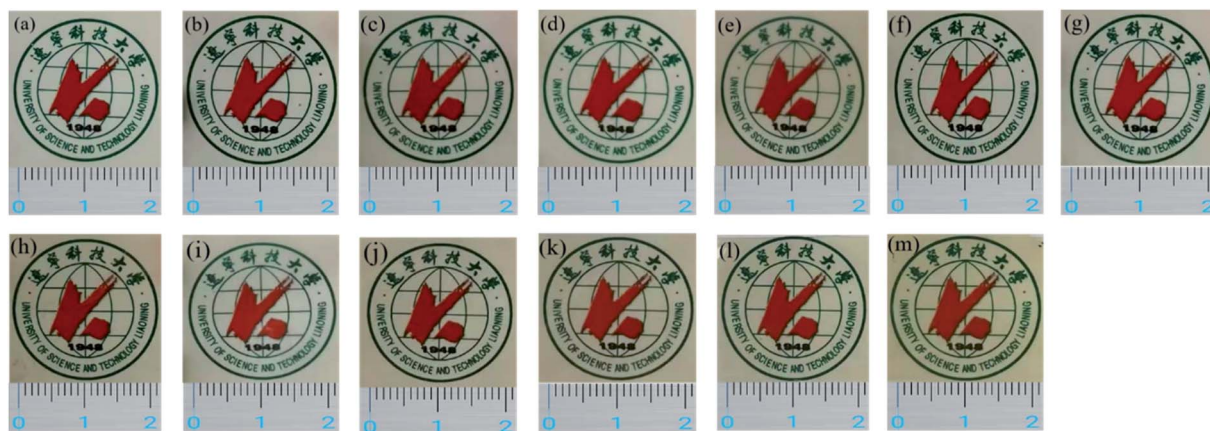**Fig. 5** TGA curves of PI and nanocomposite films.

Fig. 6 Images of triarylimidazole-containing PI and nanocomposite film (a) PI(MPBAI-CBDA), (b) PI(SiO$_2$-0.02%), (c) PI(SiO$_2$-0.10%), (d) PI(SiO$_2$-0.50%), (e) PI(SiO$_2$-2.50%), (f) PI(Al$_2$O$_3$-0.02%), (g) PI(Al$_2$O$_3$-0.10%), (h) PI(Al$_2$O$_3$-0.50%), (i) PI(Al$_2$O$_3$-2.50%), (j) PI(Si$_3$N$_4$-0.02%), (k) PI(Si$_3$N$_4$-0.10%), (l) PI(Si$_3$N$_4$-0.50%), (m) PI(Si$_3$N$_4$-2.50%).

be seen that the T_g value of PI(MPBAI-CBDA) film is about 292.2 °C, which could be explained by the improvement of chain segment movement ability due to the existence of flexible –O– linkages. With the increase of nanofillers, the T_g values of three kinds of nanocomposite films increase first and then decrease, but the change trends are slightly different. In the SiO$_2$/PI nanocomposites, when the loading of nano-SiO$_2$ is 0.50%, the T_g increases to 317.1 °C. In the Al$_2$O$_3$/PI nanocomposites, the T_g sharply increases to 317.1 °C with a nano-Al$_2$O$_3$ content of 0.02%. When the content of nano-Si$_3$N$_4$ is 0.02%, the maximum value of T_g reaches 310.6 °C. By comparison, the effect of nano-SiO$_2$ and Al$_2$O$_3$ on the T_g of nanocomposite films is more significant. In general, the interaction between the two phases and the dispersion of nanoparticles in the polymer matrix will have important impacts on the thermal properties.[50] The tight interaction limits the free rotation and movement of macromolecular segments, resulting in the increase of T_g. However, with the increase of nanoparticles, the agglomeration is easy to occur, so the interaction between macromolecules is weakened, leading to the decrease of T_g value. Thus, the introduction of nanoparticles changes the movement ability of PI segments. A proper loading of nanoparticles could effectively boost the T_g of PI films.

As shown in Fig. 5, the TGA curves of triarylimidazole-containing PI and nanocomposite films show extremely similar weight loss process. These films exhibit a main weight
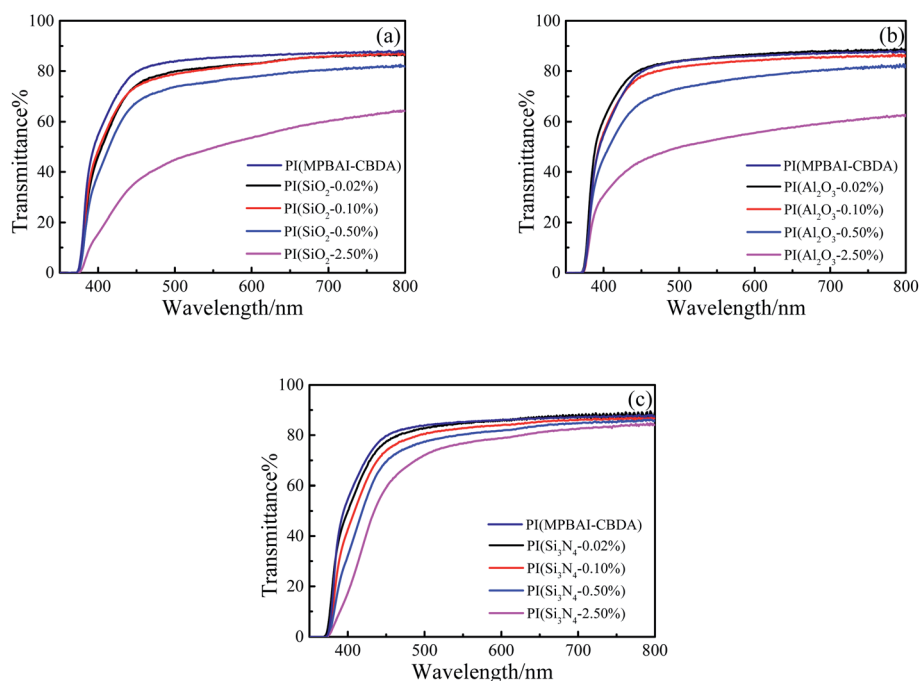

Fig. 7 UV-visible spectra of triarylimidazole-containing PI and nanocomposite films.

loss at about 420 °C, and the low thermal decomposition temperatures are chiefly caused by the fracture of alicyclic structures in PI backbones at high temperature. When the content of nanoparticles is relatively high, the T_{d5} and T_{d10} of nanocomposite films show a decline trend. As we know, the nano-SiO$_2$, Al$_2$O$_3$ and Si$_3$N$_4$ possess excellent thermal conductivity, so the energy transfer is faster and more uniform in the polymer matrix, which accelerates the decomposition of PI main chains in the heating process. Moreover, the different heat carriers for ceramics nanoparticles and organic polymer materials will lead to significant scattering of carriers at the interface.[51]

3.4 Optical properties

As we all know, colorless and transparent PI films have a unique application prospect in the field of optics. Reducing the formation of CTC and the content of conjugated structures is an effective method often used to prepare transparent PI films. The images of triphenylimidazole-containing PI and nanocomposite films are demonstrated in Fig. 6, and the UV-visible spectra and optical data are depicted in Fig. 7 and Table 2. The light transmittance and fluorescence were tested in the form of film samples, without dissolved in solvent, which is more in line with the practical application. As can be seen that the as-prepared PI(MPBAI-CBDA) film displays excellent optically transparent properties due to the presence of bulky triphenylimidazole and alicyclic structures. Owing to the large volume of triphenyimidazole groups, the distance between PI molecular chains is increased, so the formation of CTC between electron donors and donors is reduced, leading to the improvement of light transmittance. Besides, the alicyclic structures weaken the conjugate effect in the PI backbones, resulting in the light color or colorless of PI films. With the addition of three kinds of nanoparticles, the light transparency of the composite films decreases gradually. The decrease of light transparency is related to the amount of nanoparticles and the uniformity of dispersion. When the content of the nanoparticles is less than 0.50%, the nanocomposite films still maintain superior optical transparency. However, the optical transmittances of the nanocomposite films with 2.50% nano-SiO$_2$ or Al$_2$O$_3$ decrease obviously, which is possibly attributed to the difference of the film thickness as well as dispersion.

It is well known that triarylimidazole structures show strong fluorescent properties in solution, but the fluorescence effect is easy to be quenched due to the accumulation of polymer macromolecular chains in the film state. Due to the existence of alicyclic structures, the charge transfer in macromolecular chains is limited. At the same time, the large steric resistance of triarylimidazole groups hinders the close packing of PI main chains. Hence, the PI(MPBAI-CBDA) film exhibits photoluminescence behavior under the excitation of ultraviolet light.[47] After respectively adding nano-SiO$_2$, Al$_2$O$_3$ and Si$_3$N$_4$, these nanocomposite films still exhibit photoluminescence performance. The photos taken in dark room and the fluorescence emission spectra are depicted in Fig. 8 and 9, and the optical data are listed in Table 2. It can be clearly observed from the images that as the content of nanoparticles increases from 0.02% to 2.50%, the luminous intensities of nanocomposite films are enhanced. Because the introduction of a large number of nanofillers enlarges the distance between the molecular chains and hinders the interaction of chains, the quenching and CTC effect are probably weakened, resulting in the increase of fluorescence intensity and quantum yield. Moreover, the three ceramics nanoparticles are solid powder, which can increase the rigidity of the composite films. The structural rigidity is conductive to increase the planarity of the PI molecule chains and enhance the conjugation degree of π-electrons. Also, the energy losses caused by radiation and deactivation, such as transitions and internal vibrations of molecules are reduced.[48] Hence, the fluorescence emission peaks of the nanocomposite films produce a red shift, at the same time the peak intensities are increased. Relatively, the enhancement degree of nano-SiO$_2$ is more obvious than that of nano-Al$_2$O$_3$ and Si$_3$N$_4$. Specially, the 2.50% nano-Si$_3$N$_4$/PI composite film exhibits significantly red shift of 85 nm. The probable reason is that the Si$_3$N$_4$ nanoparticles as a type of semiconductor materials change the

Table 2 Optical and photoluminescence data of triarylimidazole-containing PI and nanocomposite films[a]

Samples	λ_{cutoff} (nm)	$T_{410\ nm}$ (%)	λ_{max}^{em} (nm)	Φ_{PL} (%)	λ_{shift} (nm)	C.I.E$_x$	C.I.E$_y$
PI(MPBAI-CBDA)	371	62	495	3.3	—	0.2471	0.4083
PI(SiO$_2$-0.02%)	369	54	480	3.6	−15	0.2476	0.3510
PI(SiO$_2$-0.10%)	372	56	480	4.5	−15	0.2422	0.3650
PI(SiO$_2$-0.50%)	372	47	485	11.7	−10	0.2470	0.3732
PI(SiO$_2$-2.50%)	374	20	520	17.2	25	0.2982	0.4259
PI(Al$_2$O$_3$-0.02%)	370	67	490	3.4	−5	0.2344	0.3780
PI(Al$_2$O$_3$-0.10%)	372	63	490	4.9	−5	0.2566	0.3869
PI(Al$_2$O$_3$-0.50%)	370	52	495	5.3	0	0.2552	0.3986
PI(Al$_2$O$_3$-2.50%)	370	34	500	6.8	5	0.2497	0.4135
PI(Si$_3$N$_4$-0.02%)	368	58	505	3.7	10	0.2539	0.3746
PI(Si$_3$N$_4$-0.10%)	372	51	525	4.8	30	0.3007	0.4123
PI(Si$_3$N$_4$-0.50%)	373	42	555	6.2	60	0.3572	0.4236
PI(Si$_3$N$_4$-2.50%)	372	26	580	8.5	85	0.4886	0.4151

[a] λ_{cutoff}: cut-off absorption wavelength; $T_{410\ nm}$: transmittance at 410 nm; λ_{max}^{em}: maximum emission wavelength; Φ_{PL}: fluorescence quantum yield; λ_{shift}: maximum emission wavelength redshift.
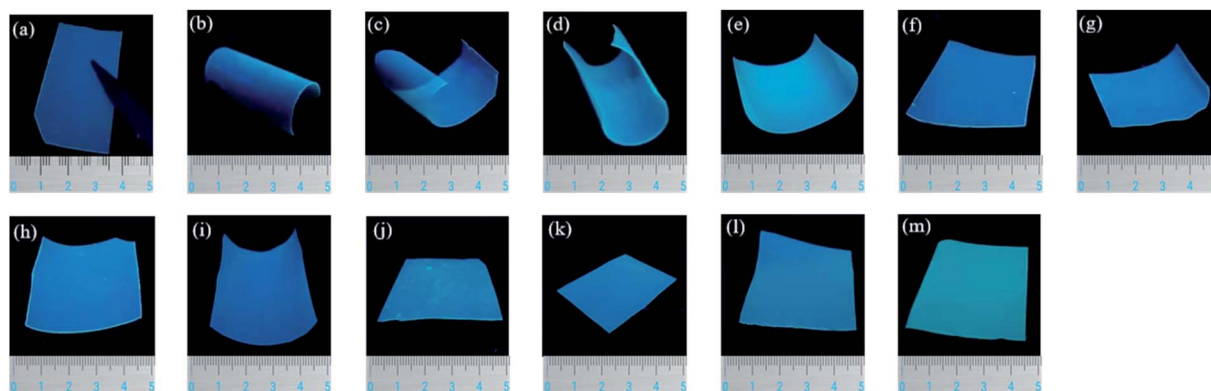
Fig. 8 Images of triarylimidazole-containing PI and nanocomposite films under 365 nm ultraviolet light (a) PI(MPBAI–CBDA), (b) PI(SiO$_2$-0.02%), (c) PI(SiO$_2$-0.10%), (d) PI(SiO$_2$-0.50%), (e) PI(SiO$_2$-2.50%), (f) PI(Al$_2$O$_3$-0.02%), (g) PI(Al$_2$O$_3$-0.10%), (h) PI(Al$_2$O$_3$-0.50%), (i) PI(Al$_2$O$_3$-2.50%), (j) PI(Si$_3$N$_4$-0.02%), (k) PI(Si$_3$N$_4$-0.10%), (l) PI(Si$_3$N$_4$-0.50%), (m) PI(Si$_3$N$_4$-2.50%).

emission energy level of the triarylimidazole-containing PI film, leading to the decline of the energy level of the first excited singlet state.[52] The functional groups on the surface of nanoparticles such as Si–OH, –OH, –NH$_2$ and Si–NH$_2$, are electron-donating groups, which can increase the transition probability between the lowest excited singlet state and the ground state. In addition, the permittivity of nano-Si$_3$N$_4$ is higher than that of nano-SiO$_2$, so the result is similar with that reported in the literature.[46] Thus, the type and content of doped nanoparticles play an important role in the photoluminescence properties of PI nanocomposite films.

According to Table 2, with the increase of nanoparticle content, the fluorescence quantum yields of nanocomposite films are improved in varying degrees. Specially, the

fluorescence quantum yield of the composites containing 2.50% nano-SiO$_2$ fillers reaches 17.2%, meaning a very noticeable improvement. Additionally, Fig. 10 gives the C.I.E 1931 chromaticity diagram calculated from the fluorescence emission spectra of nanocomposite films, and the corresponding color coordinate values are also shown in Table 2. It is found that the nano-Si$_3$N$_4$ particles take the greatest influence on chromaticity of composite films, while the nano-Al$_2$O$_3$ fillers have the least effect on chromaticity. Therefore, the properties of inorganic nanofillers may be responsible for this result.

3.5 Surface property and water absorption

When the PI film materials are used in the field of microelectronics and optoelectronic, the hydrophobic property of the
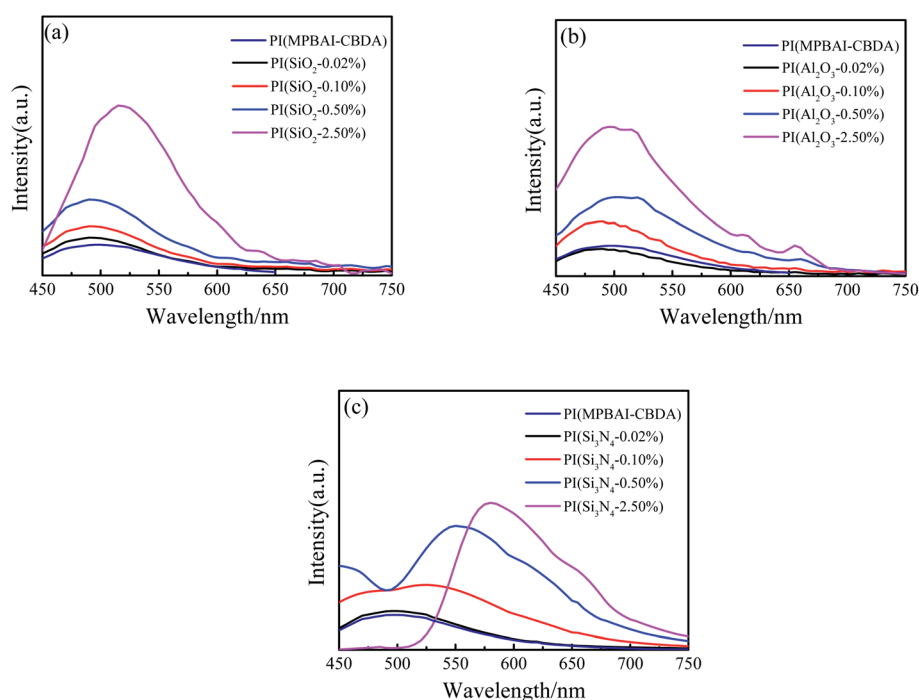

Fig. 9 Emission spectra of triarylimidazole-containing PI and nanocomposite films excited at 425 nm (a) PI(nano-SiO$_2$); (b) PI(nano-Al$_2$O$_3$) (c) PI(nano-Si$_3$N$_4$).
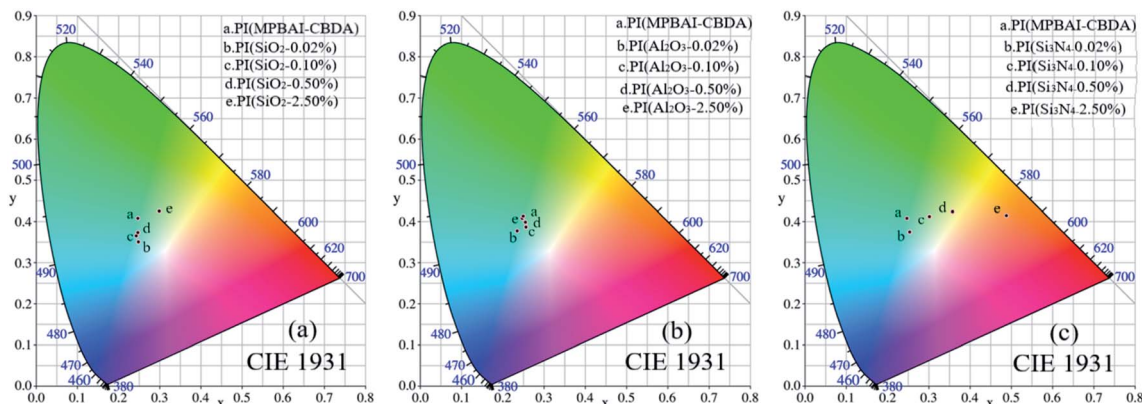
Fig. 10 C.I.E-1931 chromaticity diagrams of triarylimidazole-containing PI and nanocomposite films (a) PI(nano-SiO₂), (b) PI(nano-Al₂O₃) and (c) PI(nano-Si₃N₄).
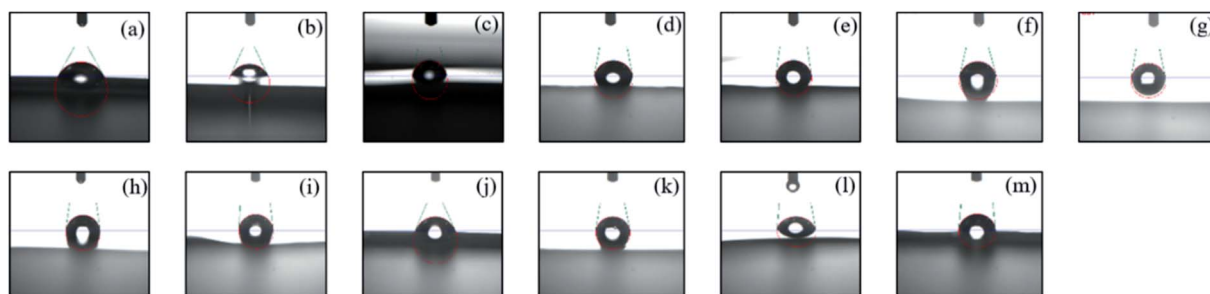

Fig. 11 Images of water contact angle on the surface of triarylimidazole-containing PI and nanocomposite films (a) PI(MPBAI-CBDA), (b) PI(SiO₂-0.02%), (c) PI(SiO₂-0.10%), (d) PI(SiO₂-0.50%), (e) PI(SiO₂-2.50%), (f) PI(Al₂O₃-0.02%), (g) PI(Al₂O₃-0.10%), (h) PI(Al₂O₃-0.50%), (i) PI(Al₂O₃-2.50%), (j) PI(Si₃N₄-0.02%), (k) PI(Si₃N₄-0.10%), (l) PI(Si₃N₄-0.50%), (m) PI(Si₃N₄-2.50%).

surface will have a great impact on the stability and reliability of the materials.[53] Fig. 11 illustrates the images of water contact angle on the surface of triarylimidazole-containing PI and nanocomposite films, and the data of contact angle and water absorption are given in Table 1. As can be seen that the spreading of water droplet on the pure PI(MPBAI-CBDA) film surface shows good hydrophilicity with a contact angle of 59°. Because the imidazole structures have good water solubility, the corresponding PI shows poor hydrophobicity, limiting its practical application. Due to the incorporation of nanoparticles, the contact angles exhibit an increasing trend, indicating that the wettability of the liquid to the film surface decreases. When the content of nano-SiO₂, Al₂O₃ and Si₃N₄ is 2.50%, the contact angles of composite films reach 81°, 84° and 85°. Based on the XRD results, the improvement of hydrophobicity is mainly attributed to the increase of structural regularity of PI films.[54] Furthermore, the water absorption increases with the increase of nanoparticles content, and the three systems show a similar trend. When the film samples are immersed in deionized water for a long time, the interface defects between inorganic particles and organic matrix may cause the infiltration of water molecules. In addition, the imidazole structures and some hydrophilic groups will also play a role in enhancing water absorption.[55] Therefore, the introduction of the three kinds of nanoparticles tends to improve the hydrophobicity of the

material surface, but is detrimental to long-term water absorption.

4. Conclusions

The diamine MPBAI containing triphenylimidazole groups was synthesized and polymerized with CBDA to prepare the colorless and transparent PI films. By virtue of *in situ* polymerization, three kinds of nanoparticles, including nano-SiO₂, Al₂O₃ and Si₃N₄ were introduced into the PI(MPBAI-CBDA) matrix to fabricate the corresponding nanocomposite films. These films showed excellent optical properties, close to colorless and transparent. With the increase of nanoparticle content, the T_g of composite films increased first and then decreased, while the thermal decomposition temperature chiefly exhibited a decline trend. Particularly, all these films displayed photoluminescence properties in film state. As the loading of nanoparticles increased, the photoluminescence intensity and the fluorescence quantum yield of nanocomposite films enhanced obviously. When the nano-SiO₂ content was 2.50%, the relative luminous intensity increased by 9.2 times, and the absolute fluorescence quantum yield was 5.2 times of pure PI(MPBAI-CBDA) films. In addition, the position of fluorescence emission peak was significantly red-shifted about 85 nm when the added nano-Si₃N₄ was 2.50% in the PI matrix. By adjusting the

type and content of nanoparticles, the fluorescence intensity and chromaticity of PI films can be effectively regulated. Besides, the introduction of three kinds of nanoparticles is conducive to improve the hydrophobicity of the film surface. Therefore, this paper reported a method to improve the photoluminescence properties of PI films containing triphenylimidazole by introducing the ceramics nanoparticle. These functional PI films are expected to be used in some special optical fields.

Conflicts of interest

There are no conflicts to declare.

Acknowledgements

References

1 G. S. Liou, P. H. Lin, H. J. Yen, Y. Y. Yu and W. C. Chen, *J. Polym. Sci., Part A: Polym. Chem.*, 2019, **48**(6), 1433–1440.

2 J. H. Chang, K. M. Park, S. M. Lee and J. B. Oh, *J. Polym. Sci., Part B: Polym. Phys.*, 2015, **38**(19), 2537–2545.

3 R. L. Han, Y. L. Xie and X. F. Ma, *Chin. J. Chem. Eng.*, 2019, **27**(4), 150–156.

4 E. Sugimoto, *IEEE Electr. Insul. Mag.*, 2002, **5**(1), 15–23.

5 K. Yokota, N. Ohmae and M. Tagaw, *J. Spacecr. Rockets*, 2002, **39**(1), 155–156.

6 B. Kraftschik, W. J. Koros, J. R. Johnson and O. Karvan, *J. Membr. Sci.*, 2013, **428**, 608–619.

7 X. D. Guo, Y. Dai, M. Gong, Y. G. Qu and L. E. Helseth, *Appl. Surf. Sci.*, 2015, **349**, 952–956.

8 B. B. Sauer and B. S. Hsiao, *Polymer*, 1993, **34**(15), 3315–3318.

9 C. H. Ju, J. C. Kim and J. H. Chang, *J. Appl. Polym. Sci.*, 2010, **106**(6), 4192–4201.

10 Y. Oishi, K. Ogasawara, H. Hirahara and K. Mori, *J. Photopolym. Sci. Technol.*, 2006, **13**(2), 323–326.

11 P. H. Li, C. Y. Wang, G. Li and J. M. Jiang, *eXPRESS Polym. Lett.*, 2009, **3**(11), 703–712.

12 D. M. Li, A. H. McDaniel, R. Bastasz and J. W. Medlin, *Sens. Actuators*, 2006, **115**(1), 86–92.

13 X. Y. Gao, L. Lin, Y. C. Liu and X. Q. Huang, *J. Disp. Technol.*, 2015, **11**(8), 666–669.

14 J. H. Chang, H. K. Ji, L. H. Quach, H. W. Kim and H. M. Kim, *IEEE Trans. Appl. Supercond.*, 2018, **99**, 1.

15 S. H. Bang, K. K. Kim, H. Y. Jung, T. H. Kim, S. H. Jeon and J. B. Seol, *Thin Solid Films*, 2014, **558**, 405–410.

16 D. Suryanarayana and K. L. Mittal, *J. Appl. Polym. Sci.*, 2010, **30**(7), 3107–3111.

17 H. Seyedjamali and A. Pirisedigh, *J. Mater. Sci.*, 2011, **46**(20), 6744–6750.

18 J. Lee, S. S. Kim, D. Kang, C. Roh and C. Kang, *Prog. Org. Coat.*, 2019, **127**, 117–123.

19 W. Leng, Y. Zhou, Q. Xu and J. Liu, *Proc. SPIE*, 2001, **4602**, 139–141.

20 H. Lu and S. Sun, *Comput. Mater. Sci.*, 2018, **146**, 119–125.

21 E. I. Mal'Tsev, M. A. Brusentseva, V. I. Berendyaev, V. A. Kolesnikov and A. V. Vannikov, *Polym. Adv. Technol.*, 2015, **11**(7), 325–329.

22 S. C. Hsu, W. T. Whang and C. S. Chao, *Thin Solid Films*, 2007, **515**(17), 6943–6948.

23 M. Ghaemy and R. Alizadeh, *Eur. Polym. J.*, 2009, **45**(6), 1681–1688.

24 X. F. Li, Y. J. Liu, H. B. Chen and H. M. Li, *Eur. Polym. J.*, 2019, **121**, 109347.

25 J. C. Jung and S. B. Park, *Polym. Bull.*, 1995, **35**(4), 423–430.

26 M. Ghaemy, F. R. Berenjestanaki and M. Bazzar, *Des. Monomers Polym.*, 2014, **17**, 101–110.

27 A. Hariharan, S. Kumar, M. Alagar, K. Dinakaran and K. Subramanian, *Polym. Bull.*, 2018, **75**, 93–107.

28 M. Lian, F. Zheng, Q. Wu, X. M. Lu and Q. H. Lu, *Polym. Int.*, 2020, **69**, 93–99.

29 F. Akutsu, M. Inoki, M. Sawano, Y. Kasashima and M. Miura, *Polymer*, 1998, **39**(24), 6093–6098.

30 Z. Rafiee and M. Rasekh, *Polym. Adv. Technol.*, 2017, **28**(4), 533–540.

31 P. Liu, P. Zhang, D. Cao, L. Gan and Y. Li, *J. Mol. Struct.*, 2013, **1050**, 151–158.

32 L. Qu, L. Tang, R. Bei, J. Zhao, Z. Chi, S. W. Liu, X. Chen, M. P. Aldred, Y. Zhang and J. Xu, *ACS Appl. Mater. Interfaces*, 2018, 11430–11435.

33 A. L. Mohamed, M. E. El-Naggar and A. G. Hassabo, *J. Mater. Res. Technol.*, 2021, **12**, 542–554.

34 D. Yang, S. Huang, M. Ruan, Y. Wu, S. Li, H. Wang, J. Zhang, H. Ma, W. Guo and L. Zhang, *J. Mater. Chem. C*, 2017, **5**, 7759–7767.

35 S. M. Tan and M. R. Johan, *Ionics*, 2011, **17**, 485–490.

36 Y. F. Yang, G. S. Gai and S. M. Fan, *Int. J. Miner. Process.*, 2006, **78**(2), 78–84.

37 L. Yuan, J. M. Russo, R. K. Kostuk and G. Barbastathis, *Opt. Lett.*, 2010, **35**(8), 1269–1271.

38 E. Vassileva and K. Friedrich, *J. Appl. Polym. Sci.*, 2010, **101**(6), 4410–4417.

39 D. Zhao, Y. Zhang, H. Gong, B. Zhu and X. Zhang, *J. Nanomater.*, 2011, 1–5.

40 F. Liu, G. Xu, J. Wu, Y. Cheng, J. Guo and P. Cui, *Colloid Polym. Sci.*, 2010, **288**(18), 1739–1744.

41 Y. V. Chernysheva, V. G. Babak, N. R. Kildeeva, F. Boury, J. P. Benoit, N. Ubrich and P. Maincent, *Mendeleev Commun.*, 2003, **13**(2), 65–67.

42 V. E. Yudin, *eXPRESS Polym. Lett.*, 2008, **2**(7), 485–493.

43 S. Tiwari, J. Bijwe and S. Panier, *Tribol. Lett.*, 2011, **42**(3), 293–300.

44 E. Chaichana, A. Ngowthanawat, O. Mekasuwandumrong, J. Panpranot, A. Shotipruk and B. Jongsomjit, *Iran. Polym. J.*, 2012, **21**(1), 51–63.

45 K. Naitoh, K. Ishii, T. Yamaoka and T. Omote, *Polym. Adv. Technol.*, 1993, **4**(4), 294–301.

46 T. Kanamori, Y. Han, D. Nagao, N. Kamezawa, H. Ishii and M. Konno, *Mater. Sci. Eng., B*, 2016, **211**, 173–177.

47 W. Bai, Z. Z. Hu, Y. H. Lu, G. Y. Xiao, H. B. Zhao, J. M. Zhu and Z. B. Liu, *RSC Adv.*, 2021, **11**, 23802–23814.

48 X. R. Guo, F. Y. Wu, Y. N. Ni and S. Kokot, *Anal. Chim. Acta*, 2016, **942**, 112–120.

49 P. Sowinski, E. Piorkowska, S. A. E. Boyer, J. M. Haudin and K. Zapala, *Colloid Polym. Sci.*, 2015, **293**(3), 665–675.

50 M. Sokolowski, Z. Parlak, C. Bartsch, S. Zauscher and M. Gradzielski, *ACS Appl. Nano Mater.*, 2019, **2**(4), 1808–1819.

51 S. Park, J. Jang, H. Kim, D. Park, K. Kim and H. J. Yoon, *J. Mater. Chem. A*, 2020, **8**, 19746–19767.

52 L. C. Estrada, O. E. Martinez, M. Brunstein, S. Bouchoule and A. M. Yacomotti, *Opt. Express*, 2010, **18**(24), 24793–24808.

53 T. Kim, C. Bao, M. Hausmann, G. Siqueira, T. Zimmermann and W. S. Kim, *Adv. Electron. Mater.*, 2019, **5**(2), 1800778–1800785.

54 S. Vafaei, T. Borcatasciuc, M. Z. Podowski, A. Purkayastha, G. Ramanath and P. M. Ajayan, *Nanotechnology*, 2006, **17**(10), 2523–2527.

55 K. Kawabe, T. Sasagawa, Y. Yoshikawa, A. Ichimura, K. Kumekawa, N. Yanagihara, T. Takino, H. Sakurai and Y. Kojima, *J. Biol. Inorg. Chem.*, 2003, **8**(8), 893–906.